Terr. Atmos. Ocean. Sci., Vol. 25, No. 4, 471-481, August 2014 doi: 10.3319/TAO.2014.02.24.01(T)

Superconducting Gravimeters Detect Gravity Fluctuations Induced by M_w 5.7 Earthquake Along South Pacific Rise Few Hours Before the 2011 M_w 9.0 Tohoku-Oki Earthquake

Keliang Zhang * and Jin Ma

State Key Laboratory of Earthquake Dynamics, Institute of Geology, China Earthquake Administration

Received 25 March 2013, revised 21 February 2014, accepted 24 February 2014

ABSTRACT

Gravity changes sometimes appear before a big earthquake. To determine the possible sources is important for recognizing the mechanism and further geodynamic studies. During the first two hours on March 11 before the M_w 9.0 Tohoku-Oki earthquake, the non-tidal gravity time series of superconducting gravimeters worldwide showed low-frequency (< 0.10 Hz) fluctuations with amplitude of ~1 to 4 × 10^{-8} ms^{-2} lasting ~10 - 20 minutes. Through comparing global seismicity with the arrival times of seismic waves, we find that the fluctuations were induced by the M_w 5.7 earthquake that occurred at 0:14:54.68 at (53.27°S, 118.18°W) along the eastern South Pacific Rise. Several body waves such as P, S are clearly recorded in the station with ~400 km distance to the hypocenter. The fluctuations are in response to the waves that propagate with a velocity of about 4 km s^{-1}. Their amplitudes are proportional to the inverse of the epicentral distances even though the fluctuations of European sites were overlapped with waves associated with a smaller, i.e., M_w 2.6, event in Europe during this period. That is, the M_w 5.7 earthquake induced remarkable gravity fluctuations over long distances at stations all over the world. As such, the foreshocks with larger magnitudes occurred before the M_w 9.0 earthquake would have more significant influence on the gravity recordings and the seismic-wave induced component should be removed during the analysis of anomalies prior to a great earthquake in future studies.

Key words: Superconducting gravimeter, Gravity change, Long-distance earthquake, Tohoku-Oki earthquake, Solid tide

Citation: Zhang, K. and J. Ma, 2014: Superconducting gravimeters detect gravity fluctuations induced by M_w 5.7 earthquake along South Pacific Rise few hours before the 2011 M_w 9.0 Tohoku-Oki earthquake. Terr. Atmos. Ocean. Sci., 25, 471-481, doi: 10.3319/TAO.2014.02.24.01(T)

1. INTRODUCTION

The Superconducting gravimeter (SG) is a spring-type gravimeter installed with a magnetic superconducting sphere that levitates within a stable magnetic field (Prothero and Goodkind 1968; Goodkind 1999). SGs were developed more than 50 years ago and have become the most sensitive and stable instrument for gravity measurement with 1 nano-Gal (1 × 10^{-11} ms^{-2}) capability in the frequency domain (an accuracy of 0.1 μgal in time domain) with a low drift rate of a few microgal per year. Thanks to the high precision SGs have been used to monitor geophysical phenomena for different periods and amplitudes, such as solid earth tide, atmospheric effects, ocean and polar motion, precipitation, groundwater changes and earthquakes (Hinderer et al. 2007; Neumeyer 2010).

Most of these long-term changes require a time window at least one day or longer. It is notable that SGs, like other types of gravimeters, are usually designed to filter out seismic "noise", and they appear difficult to record large seismic waves faithfully due to the limited dynamic range. As a result, earthquake-related disturbance signals lasting hours are usually first removed as noise in the data preprocessing. In comparison, the best SG sites are less noisy than long-period seismometers below 1 mHz (Rosat and Hinderer 2011) and thus SGs are useful tools for detecting the Earth's free oscillations with periods longer than 500 s excited by large earthquakes. SGs have recorded a series of co-seismic gravity responses (Imanishi et al. 2004; Hwang et al. 2009; Kim et al. 2009) as well as some early body phases and Rayleigh phases induced by earthquakes (Kamal and Manisinha 1992; Imanishi et al. 2004), comparable to those by seismometers.

* *Corresponding author*
E-mail: keliang_zhang@hotmail.com

Therefore, SGs might have the ability to provide complementary data to seismometers for earthquake studies as gPhone (Niebauer et al. 2011) in the cases that the waves magnitudes are within the range of measurement.

SGs have recently recorded gravity perturbation phenomena that started several days before large earthqaukes. During the perturbation the amplitude of the gravity time series increases prior to the earthquake and gradually decreases after the earthquake (Lan et al. 2011; Shen et al. 2011). Such phenomena have been detected with SG data during several large earthquakes such as the 2004 M_w 9.3 Sumatra earthquake (Wang et al. 2007), the 2008 M_w 7.9 Wenchuan earthquake (Shen et al. 2011) and some smaller ones (Lan et al. 2011). Before the M_w 9.0 Tohoku-oki earthquake, similar anomalies appeared in 5-day (March 6 - 11, 2011) recordings in SGs (Zhang et al. 2013) and gPhone gravimeters (Wei et al. 2011). Meanwhile, during that period, several hundreds small earthquakes migrated to and finally stopped near the hypocenter of the mainshock along the trench (Kato et al. 2012). The accumulated quasi-static slip near the hypocentral area increased abruptly from a constant of ~5 to ~12 cm within about six hours before the mainshock. The slip change was also confirmed by GPS observations (Miyazaki et al. 2011; Suito et al. 2011). As such, the temporal process of gravity changes is, to some extent, comparable to the migrating evolution of foreshock sequences (Miyazaki et al. 2011; Kato et al. 2012). There would be a fast loading process during the relatively short period. By far, there is no evidence to suggest whether the perturbation is related to the seismicity migration. Is there any response to the transition process in the SGs time series?

In this study, we first examined whether abrupt gravity changes or fluctuations existed during the first few hours on March 11, and then discussed the possible sources and finally found that the gravity fluctuations resulted from an M_w 5.7 earthquake. Thus, the gravity fluctuation due to long-distance earthquakes with magnitudes larger than 6 would be more carefully focused when the pre-seismic perturbation signals are extracted as many researchers have realized (Lan et al. 2011; Shen et al. 2011; Zhang et al. 2013).

2. DATA PROCESSING

Since the M_w 9.0 Tohoku-Oki earthquake occurred, the Global Geodynamic Project (GGP, http://www.eas.slu.edu/GGP) has released 1 Hz sampling data from 21 SGs (i.e., 18 stations, since there are 3 sensors in Bad Homberg and 2 sensors in Wettzell, respectively. Table 1, Figs. 1a, b) spanning the whole period of March, 2011.

The first step is to remove the theoretical solid tide and instantaneously observed atmospheric pressure effect (Hinderer et al. 2007). We employed the modified program g1sres.f which is released on the GGP website (http://www.eas.slu.edu/GGP/snm.html). In the calculation the potential by Xi (1987) is chosen with a cut-off of 0.0001, yielding 383 waves with precision of 0.04×10^{-8} ms^{-2}. Although ocean tides can be added to the potential, this will be station dependent and the inclusion of ocean tides would not affect the noise level in the seismic band (Banka and Crossley 1999). In addition, we subtracted the atmospheric pressure effect with a simple admittance of -0.3×10^{-8} ms^{-2} mbar^{-1} as proposed by Banka and Crossley (1999).

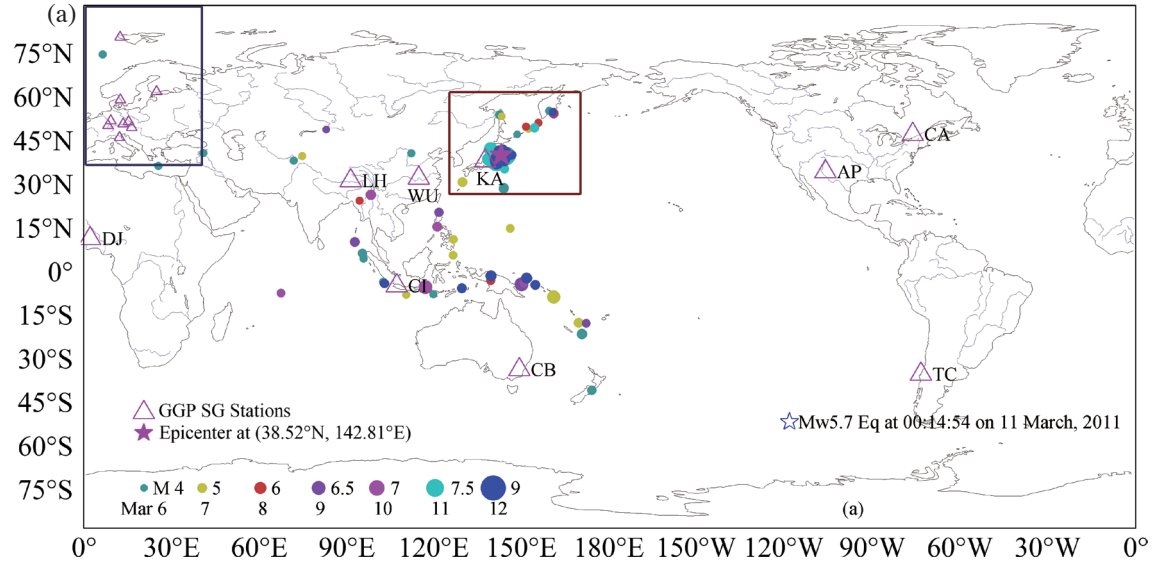

Fig. 1. Superconducting gravimeter stations (Table 1) and seismicity from 6 March to 12 March. (a) Global stations and seismicity ($M \geq 4$); (b) European stations (inset region of Fig. 1a with frame in blue) and regional seismicity ($1.2 \leq M \leq 4.4$). Solid red star and open blue star are the epicenters of the M_w 9.0 Tohoku-Oki earthquake and the M_w 5.7 eastern South Pacific Rise earthquake, respectively. Station abbreviations are detailed in Table 1.

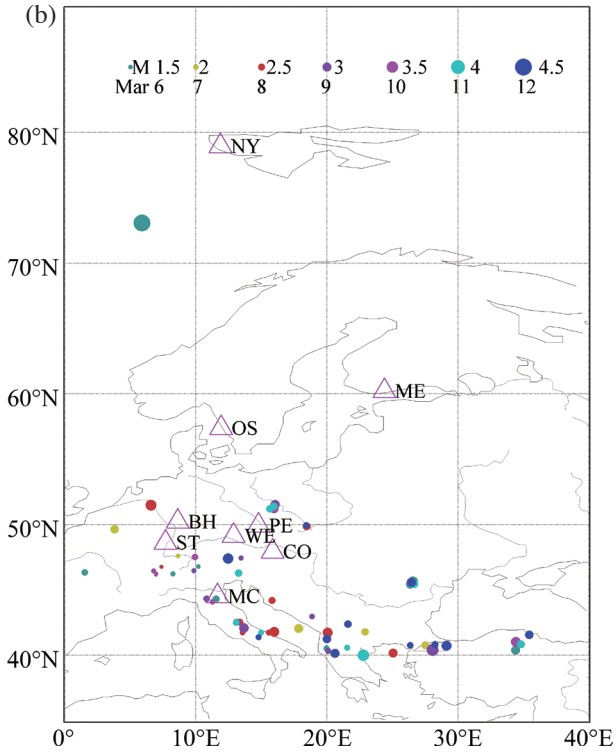

Fig. 1. (Continued)

Table 1. Observational parameters for 21 superconducting gravimeters worldwide.

Code	Station Name	Longitude (°E)	Latitude (°N)	Elevation (m)	Time delay (s)	Gravity Calibration (10^{-8} m s^{-2} V^{-1})	Instrument
AP	Apache Point, USA	-105.820	32.780	2788.00	1.54	-78.43	OSG046
CA	Cantley, Canada	284.192	45.585	269.20	12.00	-78.48 [a]	T012TT70
CB	Canberra, Australia	149.007	-35.320	762.75	37.39	-75.792	C031
CI	Cibinong, Indonesia	106.850	-6.490	138.00	8.16	-75.82	C022
CO	Conrad Observatory, Austria	15.860	47.928	1044.10	8.70	-77.95 [b]	C025
DJ	Djougou, Benin	1.606	9.742	483.00	1.54	-70.98	O060
H3	Bad Homburg, Germany	8.611	50.229	190.00	10.09	-76.68	SG044
H4	Bad Homburg, Germany	8.611	50.229	190.00	14.93	-77.59	CD029_L
H5	Bad Homburg, Germany	8.611	50.229	190.00	14.17	-81.66	CD029_U
KA	Kamioka, Japan	137.308	36.425	358.00	8.16	-58.04	T016
LH	Lhasa, China	91.035	29.645	3632.30	1.54	-77.56 [c]	SG057
MC	Medicina, Italy	11.645	44.522	28.00	11.10	-75.15	C023
ME	Metsahovi, Finland	24.396	60.217	55.60	9.48	-110.70	T020
NY	Ny-Alesund, Norway	11.867	78.930	43.00	8.16	-70.54	C039
OS	Onsala, Sweden	11.927	57.386	7.00	1.54	-77.44	054
PE	Pecny, Czech	14.785	49.913	534.58	8.86	-73.35	OSG-050
ST	Strasbourg, France	7.684	48.622	180.00	8.20	-79.20	C026
TC	TIGO Concepcion, Chile	-73.025	-36.843	156.14	10.10	-71.93	RT038
W4	Wettzell, Germany	12.878	49.144	613.70	13.40	-73.90	CD030_L
W5	Wettzell, Germany	12.878	49.144	613.70	13.40	-67.85	CD030_U
WU	Wuhan, China	114.490	30.516	80.00	35.00	-84.66 [d]	T004TT70

Note: Pressure Calibration (mbar V^{-1}): a, 60; b, -133.29; c, 100; d, 557.254; remaining stations, 1.

We subsequently estimated the Power spectral density (PSD) of the residual gravity time series using Welch's averaged periodogram spectral estimation method; in the process a 50% overlapped 1024 s Hanning window is convolved with the time series. Band-pass filtering was used to extract the specific frenquency band signal component.

3. RESULTS

Figure 2a shows the M-t diagram for 17 earthquakes with M ≥ 4 through March 10 to the initiation of the mainshock. The down arrow and the number denote the time for each earthquake as shown in Table 2. One M 6.5 and three earthquakes ~M 5 occurred within 8 hours before the mainshock (Table 2). Figure 2b shows the gravity correction for the Lhasa station during this period. The synthetic solid tide fits the observation very well, while the amplitude of the atmospheric effect is too small (< 1×10^{-8} ms^{-2}) to be directly distinguished. Figures 2c and d show the residual gravity for the period from March 10 and 11 to the mainshock, respectively. Figure 2c shows that the residual gravity was sensitive to earthquakes of M ≥ 5 globally, that is, gravity fluctuations occurred following the numbered eathquakes in Fig. 2c. Nevertheless, there was no obvious gravity response to the M 4.9 earthquake occurring at (47.83°N, 154.21°E) 4:28:19 March 11 (Figs. 2a, c). On the contrary, the time series presented a low-frequency signal with magnitude of 2 to 3×10^{-8} ms^{-2} within ~4 - 5 hours before the mainshock (UTC 0:00 - 1:00, March 11). After a comprehensive comparison (Fig. 3), we found that all of these 20 SG time sereis showed similar changes lasting 1 - 2 hours with different magnitudes (1 to 25×10^{-8} ms^{-2}). However, there seems no M ≥ 4 earthquakes occurred during this period (Fig. 2). Are these anomalies associated with the mainshock or resulting from seismicity before the mainshock?

To examine this we rearranged the time series from different stations as a function of the distance to the M_w 9.0 earthquake (Fig. 3). It shows that there is no relationship between the distance and the beginning time of the changes. For example, the anomaly for the nearest station KA arrived much later than that of the farthest TC station, indicating that the changes are not likely related to the mainshock. In

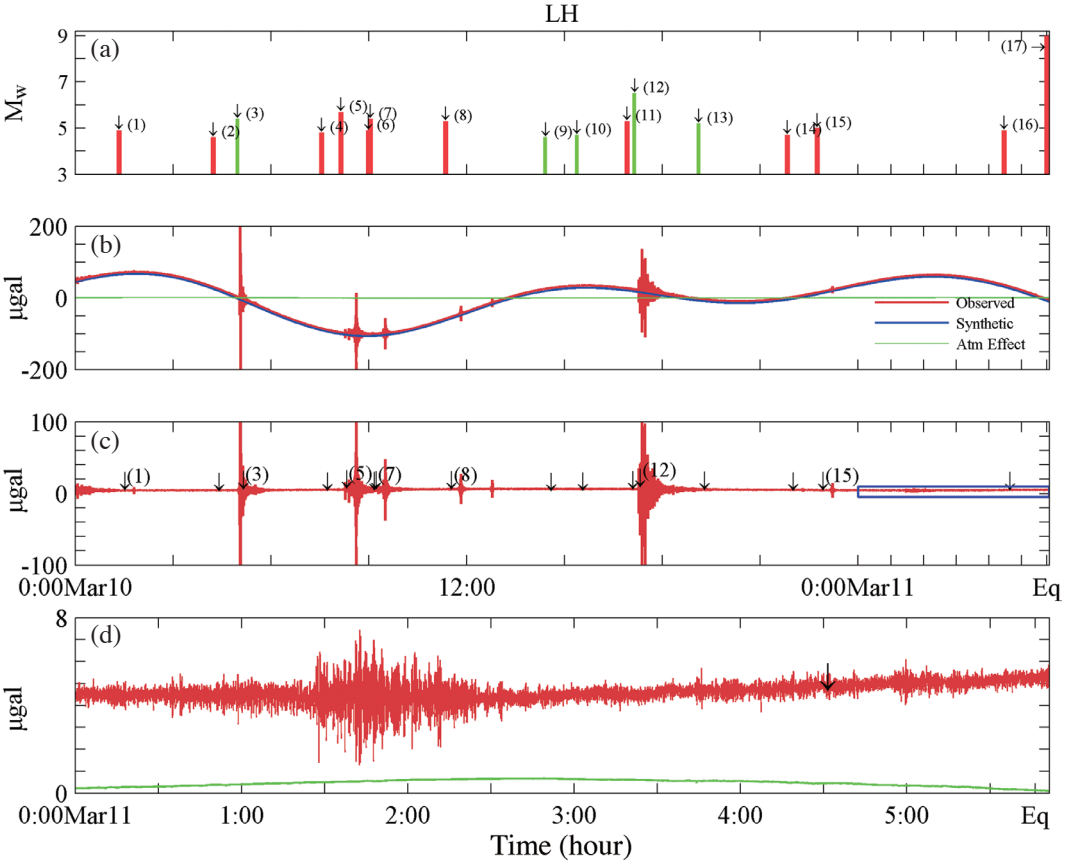

Fig. 2. Comparison between the seismicity and gravity time series for the Lhasa station. (a) M-t diagram for global seismicity (earthquakes occurring in Japan and its surroundings, i.e., red rectangular region in Fig. 1a, are shown in red and those out of the region in green); (b) Superconducting gravity data, synthetic solid tide and pressure effect for 17 hours before the mainshock; (c) Residual gravity; (d) Residual gravity during the first five hours on 11 March before the mainshock as blue rectangular region shows. The amplitude of the pressure effect during the period is less than 1, which is too small to be directly detected in Fig. 2b while it can be seen in Fig. 2d. 'Eq' of abscissa denotes the original time of M_w 9.0 earthquake, which is UTC 5:46:23 on 11 March, 2011.

Table 2. Seismicity catalog from EMSC (the European- Mediterranean Seismological Center).

List	Date	Time	Location			Magnitude
			Latitude (°N)	Longitude (°E)	Depth (km)	
1	2011.03.10	01:20:22	38.42	143.14	20	4.9
2	2011.03.10	04:13:58	38.46	143.35	20	4.6
3	2011.03.10	04:58:14	24.80	98.01	10	5.4
4	2011.03.10	07:33:05	39.04	142.47	30	4.8
5	2011.03.10	08:08:19	38.59	143.34	10	5.7
6	2011.03.10	08:59:17	38.58	143.32	10	4.9
7	2011.03.10	09:02:21	38.70	143.12	18	5.4
8	2011.03.10	11:21:08	38.66	142.98	19	5.3
9	2011.03.10	14:24:46	-5.62	150.61	113	4.6
10	2011.03.10	15:22:50	-8.95	67.07	10	4.7
11	2011.03.10	16:54:44	38.10	143.32	2	5.3
12	2011.03.10	17:08:38	-6.90	116.73	533	6.5
13	2011.03.10	19:06:13	13.81	120.74	148	5.2
14	2011.03.10	21:49:46	38.58	143.16	28	4.7
15	2011.03.10	22:44:25	38.85	143.07	30	5.0
16	2011.03.11	1:06:22	46.29	13.26	9	2.6
17	2011.03.11	4:28:19	47.83	154.21	31	4.9
18	2011.03.11	5:46:23	38.30	142.50	22	9.0

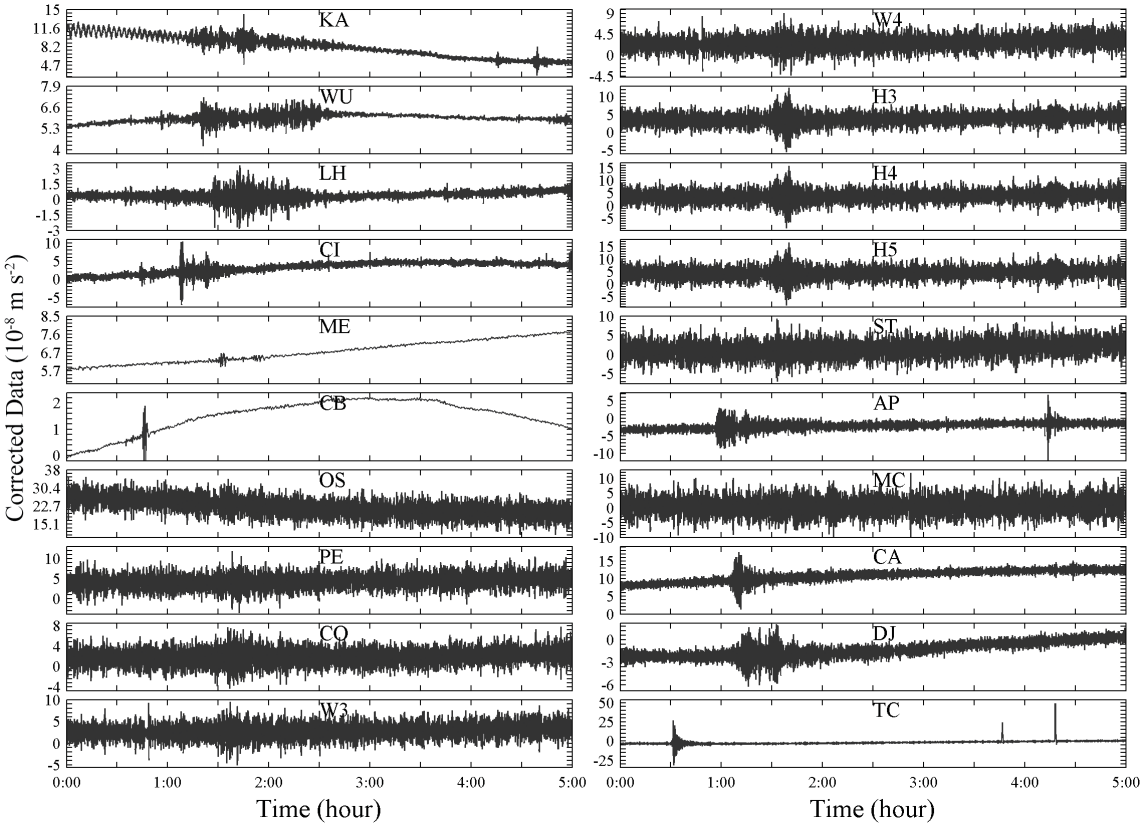

Fig. 3. Residual gravity time series of 20 SGs during the first 5 hours on March 11 arranged with distance to the M_w 9 event. Station abbreviations are detailed in Table 1. H3, H4, and H5 are in Bad Homberg; W3 and W4 are in Wettzell.

addition, the distance-sorted anomalies for the other earthquakes in Table 2 also do not have a functional relationship with the arrival time. Thus, the fluctuation might be caused by unknown (or missed) earthquake (s) or other natural events.

We further searched the global seismicity catalog (www.globalcmt.org) and found that an M_w 5.7 earthquake occurred along the eastern South Pacific Rise (53.27°S, 118.18°W) at 0:14:54.68 on March 11 (Fig. 1a, Table 3). A clear relationship apears between the beginning time and the distance from the stations to the M_w 5.7 event (Fig. 4), that is, the farther the station is to the earthquake, the later the gravity change presents.

The normalized PSD (Fig. 5) shows that most of the gravity recordings within this period have two frequency bands, 6 mHz - 0.10 Hz and 0.10 - 0.20 Hz. As we also take the results from the Lhasa station for example (Fig. 6a), the lower frequency band signal (Fig. 6b) is dominantly related to the seismic wave and the largest amplitude of fluctuation is within the dynamic range of the instrument as well. The higher frequency signal (Fig. 6c) is much more complicated and the possible sources will be discussed in a future study. The time series showing only a single frequency band are likely due to the anti-aliasing filter in the instrument system (Hinderer et al. 2007; Neumeyer 2010).

We separated the remaining time series into two frequency bands using band-pass filtering and simultaneously estimated the arrival times of all possible (converted) body wave phases with TauP (Crotwell et al. 1999; http://www.seis.sc.edu). Figure 7 shows the 25 min SG time series for the TC station. Several waves such as P, PcP and S can be

Table 3. Global CMT Catalog.

Date	Time	Location			M	NP1			NP2			T			N			P			exp
		Lat	Long	Depth		Str	Dip	Slip	Str	Dip	Slip	Va	Pl	Az	Va	Pl	Az	Va	Pl	Az	
2011.03.11	0:14	-53.27	-118.18	16	5.7	200	80	-2	291	88	-170	4.15	5	65	-0.28	80	303	-3.87	9	156	24
2011.03.11	5:46	37.52	143.05	20	9.1	203	10	88	25	80	90	5.3	55	295	0.01	0	205	-5.32	35	115	29

Note: Global CMT refers to the Global Centroid-Moment-Tensor (CMT) Project. Abbreviations: Lat, Latitude; Long, Longitude; Str, Strike; Pl, Plunge; Az, Azimuth; M, Magnitude; exp, exponent. Unit: Lat (°N), Long (°E), Depth(km), Str(°), Dip(°), Slip(°), Pl(°), Az(°).

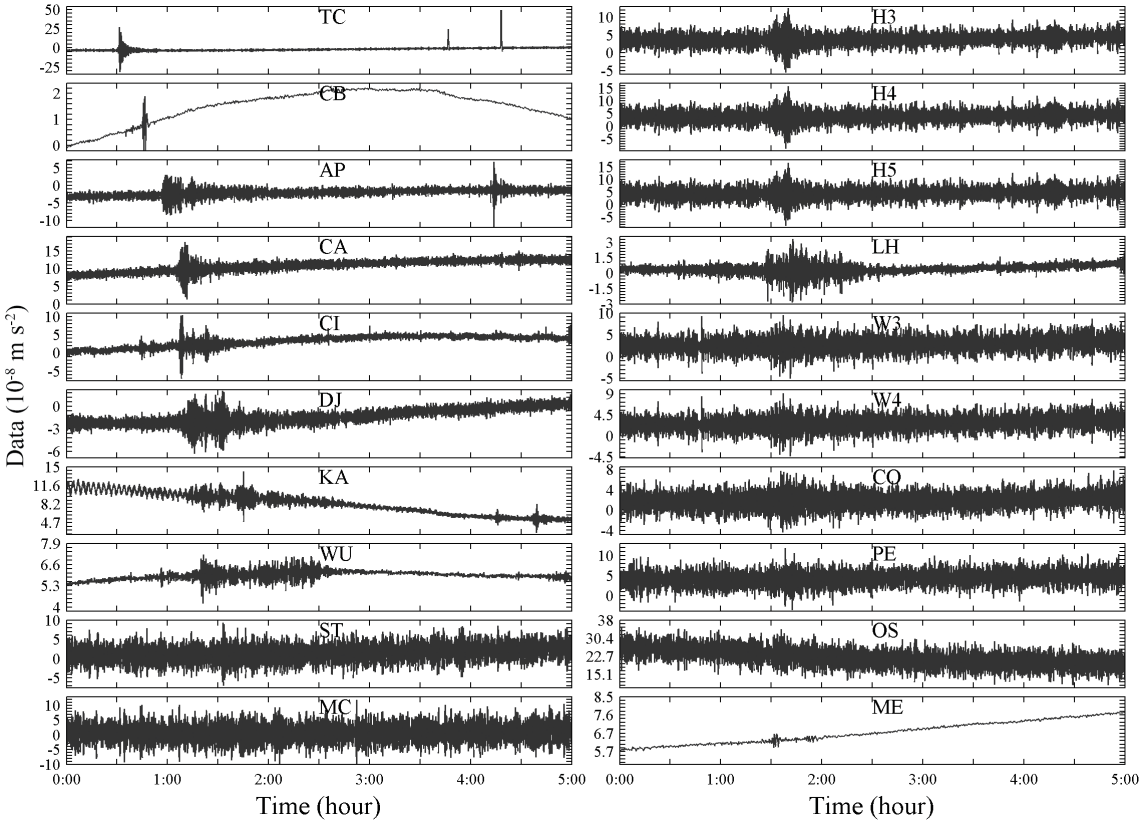

Fig. 4. Residual gravity time series of 20 SGs during the first 5 hours on 11 March before the mainshock rearranged with distance to M_w 5.7 earthquake.

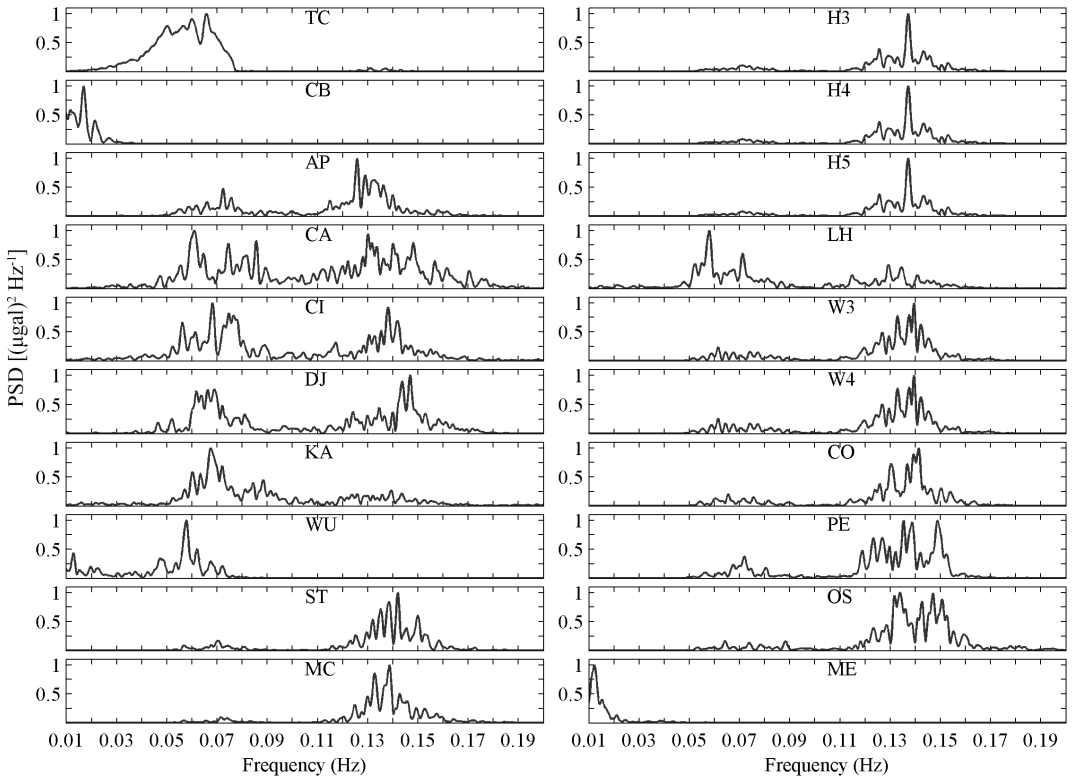

Fig. 5. Power spectral density (normalized) of the first 5 hours data on March 11 for 20 SG gravity time series. During the calculation of each PSD, a 50% overlapped Hanning window of 1024 s is convolved with the time series.

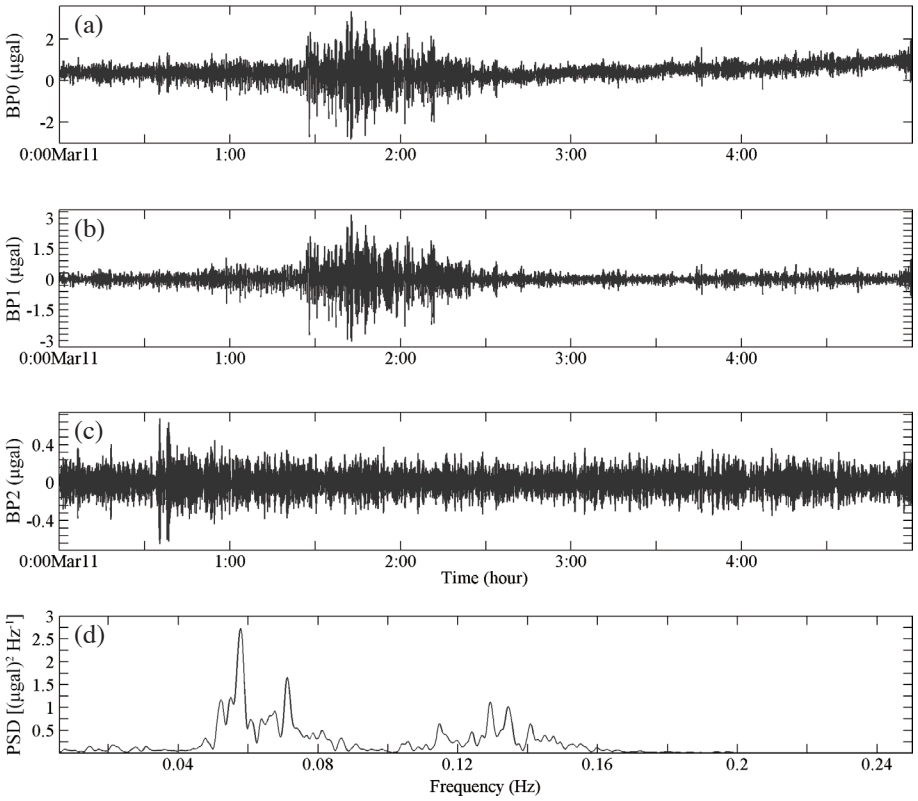

Fig. 6. Residual gravity, band pass filter results and Power spectral density of the first 5 hours data on March 11 at Lhasa station. (a) BP0, i.e., residual gravity, the same as Fig. 2d; (b) BP1 (6 mHz - 0.10 Hz); (c) BP2 (0.10 - 0.20Hz); (d) PSD for residual gravity. The PSD was calculated with a subdivision length of the gravity residuals of 5 hours, an overlapping of 50% and the data were multiplied with a 1024 s Hanning window.

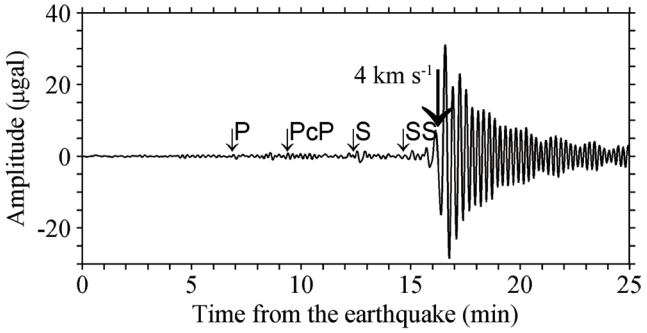

Fig. 7. A 25 min plot of band-pass filtered SG time series at TC station showing the arrival times of some early body waves and a wave with velocity of ~4 km s^{-1} after the M_w 5.7 earthquake.

recognized on the record. There are 8 more arrival phases, pP, sP and six PPs between P and PcP from the theoretical calculation, however, their amplitude is not as large as P and thus not shown. Figure 8a shows the lower band-pass filtering results and the arrival time of body waves (inverse triangles). It showed that the P wave is recorded only at the three nearest stations while for the remaining stations the first arrival is a diffracted P wave since all of these stations fall in the shadow zone. Except for the TC station (Fig. 7), it is hard to detect the P waves of the other two stations since the amplitudes are too small in the time series (Fig. 8). So does the diffracted P waves for the remainder time series. As the stations in Europe are relatively near to each other, the time series are overlapped together which are difficult to check, so we plotted them in Fig. 8b. The purple dashed line in Figs. 8a - b also mark the approximate arrival time of the ~4 km s^{-1} wave. It is notable that an M_w 2.6 event occurred at (46.29°N, 13.26°E) (Table 2) before the arrival of the ~4 km s^{-1} wave. Its body waves and ~4 km s^{-1} wave cover the time span of peaks from the European stations and some other far-field stations as well, such as LH, WU, KA, CI (Fig. 8), of which the amplitudes are too small to be distinguished. Thus, each time series is a combination of seismic waves due to the M_w 5.7 and the M_w 2.6 earthquakes as well as some certain noises from unknown sources.

4. DISCUSSION AND IMPLICATIONS

To determine the possible sources of gravity changes is essential for extracting meaningful geodynamic signals from a gravity time series. A recent study reported that a preseismic anomaly appeared before the M_w 9.0 Tohuku-oki earthquake (Zhang et al. 2013). The maximal amplitude of the anomaly can get up to ~5×10^{-8} ms^{-2}, comparable to (or even larger than) the amplitudes of the seismic-induced signals in this study. As such, the pre-seismic anomaly would be significant noise for interpreting the gravity changes a few hours before the M_w 9.0 Tohuku-oki earthquake. In fact, the pre-seismic anomalies have been reported using different types of instruments including seismometer, tiltmeter and gravimeter as well (Hao and Hu 2008; Zhang et al. 2008; Hu et al. 2010; Shen et al. 2011). However, the dominant frequencies of pre-seismic anomalies are higher than 0.10 Hz, and the frequency of seismic-related signals is below 0.10 Hz which is as same as in this study.

We compared the amplitude variations with the azimuth and distance distribution of stations with respect to the epicenters of M_w 5.7 and 9.0 earthquakes (Figs. 9a, b). The European stations are nearly located in directions of azimuth less than 30° and 45° with respect to the T-axes of M_w 5.7 and 9.0 earthquakes, respectively. We further calculated the amplitude of each low frequency time series with Fast Fourier Transformation and compared with the azimuths and distances to these two events (Figs. 9c - f). As the azimuths are distributed unevenly (Figs. 9c, e), there is no dominant direction for either the M_w 5.7 or 9.0 earthquake from just 20 stations even though the amplitude of TC is the largest. In comparison, the amplitude is proportional to the inverse of distance to the M_w 5.7 event (Fig. 9d) while no such relationship was found for the M_w 9.0 earthquke (Fig. 9f). Since only 17 sites are used in this study and these stations are not evenly distributed in space, it is hard to find a dominant direction that might have significant influence on the amplitude as suggested by Lan et al. (2011). Nevertheless, the amplitude dependence on the epicentral distance is much more valid and not vulnerable to be affected by either a smaller local earthquake or complex of large scale tectonic loading (Ma et al. 2007; Kennett et al. 2011; Tajima et al. 2013).

Thus, the low-frequency gravity changes are fluctuation responses to seismic waves, with averaged velocity of ~4 km s^{-1} (downward arrows, Fig. 8), induced by the M_w 5.7 earthquake rather than either pre-seismic anomalies or the oceanic noise, which also has two dominant peaks at 5 - 6 and 10 - 15 s (Longuet-Higgins 1950; Hinderer et al. 2007). The fluctuations are neither likely response to the accelerating process nor foreshocks before the M_w 9.0 earthquake (Ando and Imanishi 2011; Kato and Yoshida 2011; Kennett et al. 2011; Kato et al. 2012; Tajima et al. 2013). Most foreshocks have magnitudes larger than M_w 5.7 and they would have influenced the gravity observations and thus need to be removed from the source detection for gravity signals with frequencies of 0.10 - 0.20 Hz.

5. CONCLUSIONS

We studied the possible source of the gravity fluctuation changes that lasted ~10 - 20 minutes within about five hours before the M_w 9.0 Tohoku-Oki earthquake. Through a global seismicity search and estimate of the arrival times of different seismic phases, we found that the gravity fluctuations were induced by the M_w 5.7 earthquake occurring at 0:14:54 at (53.27°S, 118.18°W) along the eastern South Pacific Rise. The frequency band of seismic-wave related

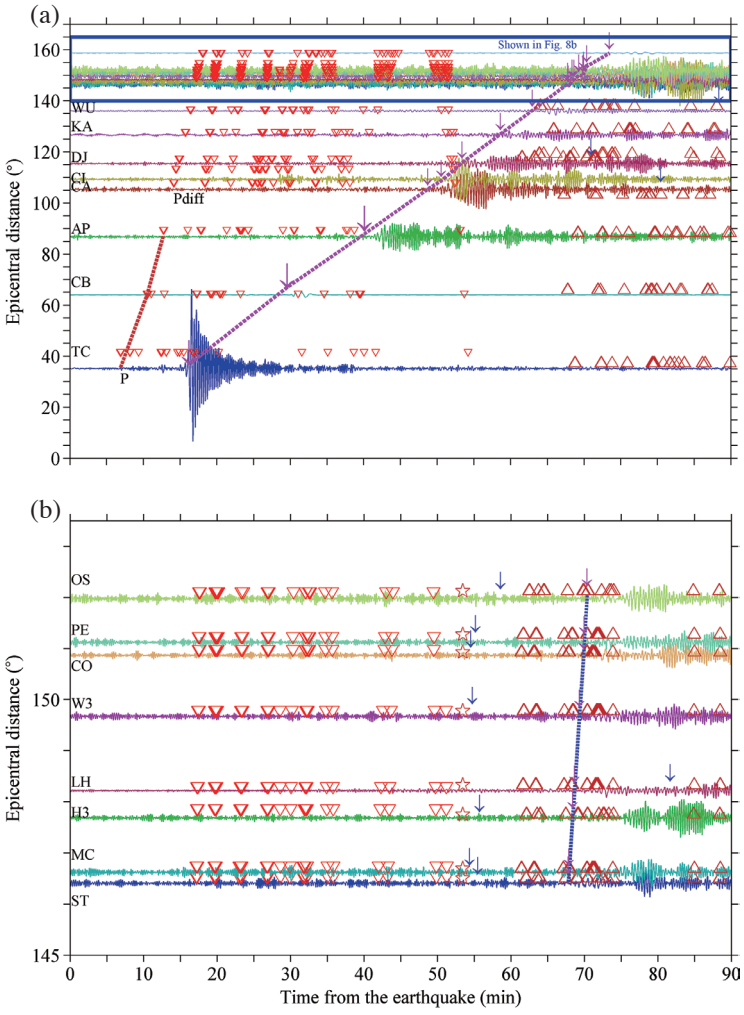

Fig. 8. Band-pass filtered (0.006 - 0.10 Hz) gravity changes during the first 1.5 hours on 11 March as function of epicentral distance (a). (b) The filtered time series for the stations farther than 140°. The first arrivals are P waves and diffracted P waves for the first three stations and the remainder, respectively. The purple dashed line denotes the arrival of waves with velocity ~4 km s^{-1}. The inverse triangles denote M_w 5.7 event and its arrival times of different phases, respectively. The star and triangles denote M_w 2.6 earthquake and its arrival times of different phases. The arrival times of waves are estimated with TauP.

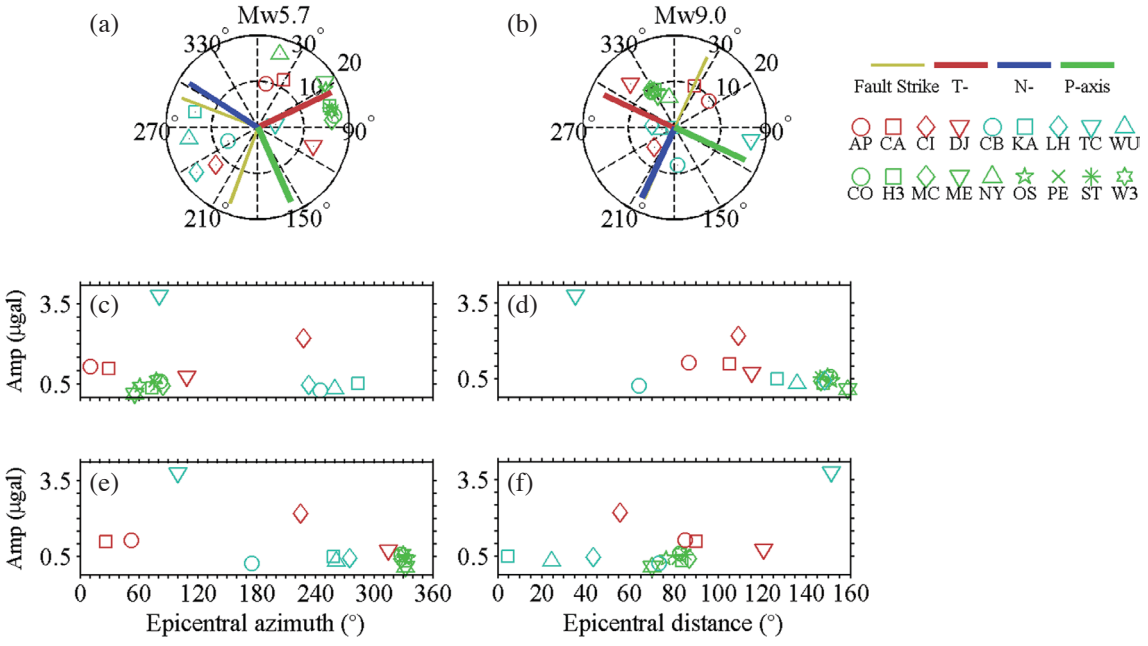

Fig. 9. Distribution of GGP Stations arranged with azimuth and distance w.r.t. M_w 5.7 earthquake (a) and M_w 9.0 earthquake (b), respectively; and fluctuation amplitudes versus epicentral azimuths (c) (e) and epicentral distances (d) (f) w.r.t. these two earthquakes, respectively.

gravity fluctuations is below 0.10 Hz and the propagation velocity of the fluctuations is up to ~4 km s^{-1}. Several body waves (P, S waves) are detectable through SG recording at least in the nearest (~400 km) station. Although an M_w 2.6 earthquake occurred before the arrival of the ~4 km s^{-1} wave to the European stations results in superimposed effect on the fluctuations, the amplitudes of the fluctuations are proportional to the inverse of the epicentral distance to the M_w 5.7 event. Nevertheless, no dominant direction resulting in the most significant changes was found since only 17 stations are used in this study.

Since an M_w 5.7 earthquake can induce remarkable gravity fluctuations at stations at distances greater than 400 km, the foreshocks with larger magnitudes before the M_w 9.0 earthquake would have more significant influence on the gravity recordings. Some previous studies suggested that the 0.10 - 0.20 Hz component was likely associated with the stress accumulation of the mainshock nucleation. However, we cannot make a general/further conclusion on the origin of such anomalies, since our analysis is focused on the lower frequency band and we used data during the first few hours before the mainshock. Thus, it is important to remove the gravity effects induced by seismic-waves for the detection of pre-seismic anomalies prior to a large earthquake in future studies.

Acknowledgements This study is partially supported by National Natural Science Foundation (NSFC, grant no. 41172180). KZ is partially supported by the Director Foundation of Institute of Geology, China Earthquake Administration (IGCEA1314), China Postdoctoral Science Foundation funded project (20110490460) and Key Laboratory of Computational Geodynamics, Chinese Academy of Sciences (No.003). The superconducting gravimetric data and synthetic solid tide program were provided by the Global Geodynamic Project (GGP, http://www.eas.slu.edu/GGP/tohoku2011.html). The global seismicity catalogs are available at the European- Mediterranean Seismological Center (www.emsc-csem.org) and the Global Centroid- Moment-Tensor (CMT) Project (www.globalcmt.org). TauP software is available at http://www.seis.sc.edu. We thank Dr. Cheng C.-.C and two anonymous reviewers for the constructive comments that greatly helped to improve this manuscript. An English Editor is thanked for polishing this manuscript.

REFERENCES

Ando, R. and K. Imanishi, 2011: Possibility of M_w 9.0 mainshock triggered by diffusional propagation of after-slip from M_w 7.3 foreshock. *Earth Planets Space*, **63**, 767-771, doi: 10.5047/eps.2011.05.016. [Link]

Banka, J. and D. Crossley, 1999: Noise levels of superconducting gravimeters at seismic frequencies. *Geophys. J. Int.*, **139**, 87-97.

Crotwell, H. P., T. J. Owens, and J. Ritsema, 1999: The TauP toolkit: Flexible seismic travel-time and ray-path utilities. *Seismol. Res. Lett.*, **70**, 154-160, doi: 10.1785/gssrl.70.2.154. [Link]

Goodkind, J. M., 1999: The superconducting gravimeter. *Rev. Sci. Instrum.*, **70**, 4131-4152, doi: 10.1063/1.1150092. [Link]

Hao, X. and X. Hu, 2008: Disturbance before the Wenchuan earthquake detected by broadband seismometer. *Prog. Geophys.*, **23**, 1332-1335. (in Chinese)

Hinderer, J., D. Crossley, and R. J. Warburton, 2007: Gravimetric methods - superconducting gravity meters. In: Schubert, G. (Ed.), Treatise on Geophysics, Vol. 3, 65-122.

Hu, X., X. Hao, and X. Xue, 2010: The analysis of the non-typhoon-induced microseisms before the 2008 Wenchuan earthquake. *Chin. J. Geophys.*, **53**, 2875-2886, doi: 10.3969/j.issn.0001-5733.2010.12.011. (in Chinese) [Link]

Hwang, C., R. Kao, C. C. Cheng, J. F. Huang, C. W. Lee, and T. Sato, 2009: Results from parallel observations of superconducting and absolute gravimeters and GPS at the Hsinchu station of Global Geodynamics Project, Taiwan. *J. Geophys. Res.*, **114**, B07406, doi: 10.1029/2008JB006195. [Link]

Imanishi, Y., T. Sato, T. Higashi, W. Sun, and S. Okubo, 2004: A network of superconducting gravimeters detects submicrogal coseismic gravity changes. *Science*, **306**, 476-478, doi: 10.1126/science.1101875. [Link]

Kamal, and L. Mansinha, 1992: A test of the superconducting gravimeter as a long-period seismometer. *Phys. Earth Planet. Inter.*, **71**, 52-60, doi: 10.1016/0031-9201(92)90028-T. [Link]

Kato, A., K. Obara, T. Igarashi, H. Tsuruoka, S. Nakagawa, and N. Hirata, 2012: Propagation of slow slip leading up to the 2011 M_w 9.0 Tohoku-Oki earthquake. *Science*, **335**, 705-708, doi: 10.1126/science.1215141. [Link]

Kato, N. and S. Yoshida, 2011: A shallow strong patch model for the 2011 great Tohoku-oki earthquake: A numerical simulation. *Geophys. Res. Lett.*, **38**, L00G04, doi: 10.1029/2011GL048565. [Link]

Kennett, B. L. N., A. Gorbatov, and E. Kiser, 2011: Structural controls on the Mw 9.0 2011 Offshore-Tohoku earthquake. *Earth Planet. Sci. Lett.*, **310**, 462-467, doi: 10.1016/j.epsl.2011.08.039. [Link]

Kim, J. W., J. Neumeyer, T. H. Kim, I. Woo, H. J. Park, J. S. Jeon, and K. D. Kim, 2009: Analysis of Superconducting Gravimeter measurements at MunGyung station, Korea. *J. Geodyn.*, **47**, 180-190, doi: 10.1016/j.jog.2008.07.008. [Link]

Lan, S. C., T. T. Yu, C. Hwang, and R. Kao, 2011: An analysis of mechanical constraints when using superconducting gravimeters for far-field pre-seismic anomaly detection. *Terr. Atmos. Ocean. Sci.*, **22**, 271-282, doi:

10.3319/TAO.2010.11.12.01(T). [Link]

Longuet-Higgins, M. S., 1950: A theory of the origin of microseisms. *Philos. T. R. Soc. A*, **243**, 1-35, doi: 10.1098/rsta.1950.0012. [Link]

Ma, J., L. Liu, P. Liu, and S. Ma, 2007: Thermal precursory pattern of fault unstable sliding: An experimental study of en echelon faults. *Chin. J. Geophys.*, **50**, 1141-1149. (in Chinese)

Miyazaki, S., J. J. McGuire, and P. Segall, 2011: Seismic and aseismic fault slip before and during the 2011 off the Pacific coast of Tohoku Earthquake. *Earth Planets Space*, **63**, 637-642, doi: 10.5047/eps.2011.07.001. [Link]

Neumeyer, J., 2010: Superconducting gravimetry. In: Xu, G. (Ed.), Sciences of Geodesy - I: Advances and Future Directions, Springer-Verlag Berlin Heidelberg, New York, 339-413, doi: 10.1007/978-3-642-11741-1_10. [Link]

Niebauer, T. M., J. MacQueen, D. Aliod, and O. Francis, 2011: Monitoring earthquakes with gravity meters. *J. Geodesy Geodyn.*, **2**, 71-75.

Prothero, W. A. and J. M. Goodkind, 1968: A superconducting gravimeter. *Rev. Sci. Instrum.*, **39**, 1257-1262, doi: 10.1063/1.1683645. [Link]

Rosat, S. and J. Hinderer, 2011: Noise levels of superconducting gravimeters: Updated comparison and time stability. *Bull. Seismol. Soc. Am.*, **101**, 1233-1241, doi: 10.1785/0120100217. [Link]

Shen, W., D. Wang, and C. Hwang, 2011: Anomalous signals prior to Wenchuan earthquake detected by superconducting gravimeter and broadband seismometers records. *J. Earth Sci.*, **22**, 640-651, doi: 10.1007/s12583-011-0215-4. [Link]

Suito, H., T. Nishimura, M. Tobita, T. Imakiire, and S. Ozawa, 2011: Interplate fault slip along the Japan Trench before the occurrence of the 2011 off the Pacific coast of Tohoku Earthquake as inferred from GPS data. *Earth Planets Space*, **63**, 615-619, doi: 10.5047/eps.2011.06.053. [Link]

Tajima, F., J. Mori, and B. L. N. Kennett, 2013: A review of the 2011 Tohoku-Oki earthquake (Mw 9.0): Large-scale rupture across heterogeneous plate coupling. *Tectonophysics*, **586**, 15-34, doi: 10.1016/j.tecto.2012.09.014. [Link]

Wang, W., L. Ma, and J. Huang, 2007: Analysis of anomaly in gravity observation before and after strong earthquakes. *Earthquake*, **27**, 53-63. (in Chinese)

Wei, J., Z. Liu, H. Hao, Y. Wu, K. Kang, B. Zhao, C. Shen, and H. Li, 2011: Gravity anomalies in before Ms9.0 earthquake in Japan observed by continuous relative gravimeter in China. *J. Geodesy Geodyn.*, **31**, 9-11. (in Chinese)

Xi, Q., 1987: A new complete development of the tidegenerating potential for the epoch J2000.0. *Bull. Inf. Marées Terrestres*, **99**, 6766-6812.

Zhang, K., J. Ma, and D. Wei, 2013: Detection of gravity anomalies before the 2011 Mw9.0 Tohoku-Oki earthquake using Superconducting gravimeters. *Chin. J. Geophys.*, **56**, 2292-2302. (in Chinese)

Zhang, Y., J. Jiang, Y. Liao, S. Li, and T. Zhong, 2008: Joint observation of long period tremor signals with broadband seismometer, tiltmeter and gravimeter. *Acta Seismologica Sin.*, **21**, 629-635, doi: 10.1007/s11589-008-0629-y. (in Chinese) [Link]